NASA TN D-159

7N-02
197175
30P.

TECHNICAL NOTE

D-159

HEAT-TRANSFER MEASUREMENTS AT A MACH NUMBER OF 2 IN THE TURBULENT BOUNDARY LAYER ON A FLAT PLATE HAVING A STEPWISE TEMPERATURE DISTRIBUTION

By Raul J. Conti

Langley Research Center
Langley Field, Va.

(NASA-TN-D-159) HEAT-TRANSFER MEASUREMENTS AT A MACH NUMBER OF 2 IN THE TURBULENT BOUNDARY LAYER ON A FLAT PLATE HAVING A STEPWISE TEMPERATURE DISTRIBUTION (NASA. Langley Research Center) 30 p

N89-71292

Unclas
00/02 0197175

NATIONAL AERONAUTICS AND SPACE ADMINISTRATION

WASHINGTON November 1959

1H

NATIONAL AERONAUTICS AND SPACE ADMINISTRATION

TECHNICAL NOTE D-159

HEAT-TRANSFER MEASUREMENTS AT A MACH NUMBER OF 2 IN THE TURBULENT BOUNDARY LAYER ON A FLAT PLATE HAVING A STEPWISE TEMPERATURE DISTRIBUTION

By Raul J. Conti

SUMMARY

An experimental investigation has been conducted at a Mach number of 2 to determine the effects of a step in wall temperature upon the heat-transfer characteristics of a turbulent, compressible boundary layer along a flat plate. A transient heating technique was used for the measurements, which were made under near-equilibrium conditions.

The wall-temperature step caused sharp increases in heat-transfer coefficient downstream of the step, which were followed by a rapid decay. A maximum increase of 90 percent was measured, and generally good agreement with a theory by Ferrari was found. The application of this theory is analyzed in the appendix and it is shown that for the conditions of the present investigation the heat-transfer coefficient given by Ferrari's theory is essentially the same as that predicted by means of incompressible-flow theories.

INTRODUCTION

Whenever a stepwise wall-temperature distribution is encountered, substantial effects upon the heat-transfer coefficient should be expected downstream of the temperature discontinuity.

Extensive work has been done at low speeds in the past (refs. 1 to 4) toward the better understanding of this phenomenon, and it has been established that the heat-transfer coefficient goes through a large (theoretically infinite) discontinuity at the location of the temperature step and gradually decreases downstream as the boundary layer adjusts to the new wall-temperature condition. Past investigations have shown the longitudinal variation (x coordinate) of heat-transfer coefficient h after the step to be of the form

$$\frac{h}{h_{is}} = \left[1 - \left(\frac{l}{x}\right)^a\right]^{-b}$$

for incompressible flow. The symbol h_{is} denotes heat-transfer coefficient for a constant temperature plate, l is the distance from the leading edge to the step, and a and b are constants.

Recently, renewed interest has been drawn to this problem, as encountered in compressible boundary layers, mainly because (1) modern vehicle configurations may include sections of different materials at different temperatures (for example, ceramics-to-metal skin joints); and (2) some transient techniques for heat-transfer measurements are based on the so-called "plug-type heat meter" where a temperature step is also present which gives rise to appreciable errors. (See ref. 2.)

L
3
7
3

The present work was undertaken to investigate this problem in supersonic flow.

SYMBOLS

c	specific heat of metal plate, $\frac{\text{Btu}}{\text{lb } ^\circ\text{R}}$
c_f	skin-friction coefficient
$\overline{c_f}$	mean skin-friction coefficient, $\frac{1}{x}\int_0^x c_f(x)dx$
h	heat-transfer coefficient for step temperature distribution, $\frac{\text{Btu}}{\text{ft}^2\text{-sec-}^\circ\text{R}}$
h_{is}	heat-transfer coefficient for constant-temperature (isothermal) distribution, $\frac{\text{Btu}}{\text{ft}^2\text{-sec-}^\circ\text{R}}$
k	thermal conductivity of air based on free-stream temperature, $\frac{\text{Btu}}{\text{ft-sec-}^\circ\text{R}}$
K_1, K_2	defined by equations (A3) and (A5), respectively

L
3
7
3

l	distance from leading edge to temperature step, ft
M	free-stream Mach number
n	reciprocal of exponent in power law for boundary-layer velocity profile
N_{Nu}	Nusselt number
$(N_{Nu})_{is}$	Nusselt number for constant-temperature (isothermal) plate, $N_{Nu} \frac{h_{is}}{h}$
N_{St}	Stanton number
N_{Pr}	Prandtl number
R	Reynolds number based on free-stream conditions and distance along plate
t	time, sec
T	temperature, $^{\circ}R$
T_o	free-stream stagnation temperature, $^{\circ}R$
T_{aw}	adiabatic wall temperature, $^{\circ}R$
T_w	wall temperature, $^{\circ}R$
T_∞	free-stream temperature, $^{\circ}R$
T'	reference temperature (from ref. 12)
x	longitudinal coordinate from leading edge, ft
z	defined by the equation $h_{is}(x) = (\text{Constant})(x^{-z})$
δ	thickness of metal plate, ft
ρ	density of metal plate, $\frac{\text{lb}}{\text{cu ft}}$
η_r	recovery factor, $\frac{T_{aw} - T_\infty}{T_o - T_\infty}$

APPARATUS

The present investigation was conducted in a Mach number 2 blowdown jet of the Gas Dynamics Branch, Langley Research Center. This is a square, 9-inch free jet with a stagnation-pressure range of 90 to 140 pounds per square inch and a maximum stagnation temperature of 150° F. The Mach number in the test area is 2.00 ± 0.02.

The surface on which heat transfer was measured was the lower inner surface of a rectangular channel mounted on an injection mechanism (fig. 1) operated by a pneumatic actuator. This mechanism was used to swing the model from a retracted position down into the airstream after operating conditions were reached in the jet. Once in position, the leading edge of the model was 1/2 inch from the end of the tunnel, and the testing surface was parallel to the airstream $1\frac{1}{2}$ inches below the center of the jet. Since the time involved in the injection operation (about 0.5 sec) was prohibitively large for the data-reduction method used, a cover was provided in order to shield the instrumented plate. During the injection process this cover was held in place by means of a vacuum and a rapid release was achieved by replacing the vacuum by a pressure.

L
3
7
3

Static-pressure measurements along the model showed that the Mach number was 2.00 ± 0.04. A slight favorable pressure gradient existed such that $\frac{\Delta M}{\Delta x} = 0.018$ per inch. Several stagnation-pressure levels resulted in a local Reynolds number range of 0.4×10^6 to 15×10^6. The stagnation temperature was about 150° F and the magnitude of the wall temperature step was approximately 40° F.

Discontinuous-Temperature Models

The discontinuous-temperature models (models 1, 2, and 3; fig. 2(a)) consisted of a fiber glass plastic flat plate 3/4 inch thick and having a fairly sharp leading edge. Leading-edge thickness was about 0.010 inch and the wedge angle was 20°. A metal strip, 2 inches wide and 0.040 inch thick and spanning the plate, was cast in the plastic at a different x-location for each model. The material of the metal strip was a bismuth-tin alloy (65-percent bismuth) having a density of 533.4 lb/cu ft, a specific heat of 0.0395 Btu/lb-°R, and a thermal conductivity of 0.0017 Btu/ft-sec-°R. This particular alloy was chosen because its thermal properties permitted a minimization of the errors arising from heat conduction in the plate and was easy to cast on the plastic. Several thermocouples were attached to the back of this metal strip as

shown in figure 2. Model 1 also had a roughness strip of three-dimensional particles 0.003 inch high near the leading edge.

Constant-Temperature Model

The constant-temperature model (model 4; fig. 2(b)) was similar to the discontinuous-temperature models except that the metal slab covered the entire surface of the plate downstream of a 0.2-inch leading-edge reinforcement made out of plastic and steel. For the short testing times used, the temperature along this model was essentially constant.

L
3
7
3

Recovery-Temperature Model

The recovery-temperature model (model 5; fig. 2(c)) had several 1/16-inch and 1/32-inch plug-type heat meters at several x-locations as shown in the figure. This model was used to measure (under steady-state conditions) the recovery temperature at the plate surface.

MEASUREMENT TECHNIQUE

A transient heating technique was used to measure the heat-transfer coefficient. For the step temperature models the technique consisted in introducing the model into the steady airstream and allowing the front plastic section to heat up to more than 90 percent of its temperature potential $\left(T_{aw} - T_{room}\right)$ whereas the instrumented metal plate, shielded by the cover, remained at room temperature. Releasing of the cover resulted in (1) an x-wise step in wall-temperature distribution and (2) a timewise step forcing function. Recording of the temperature-time history of the thermocouples on a high-speed oscillograph during the subsequent heating of the plate permitted the evaluation of the heat-transfer coefficient by means of the following equation:

$$h = \rho c \delta \frac{\partial T_w / \partial t}{T_{aw} - T_w} \tag{1}$$

The recovery temperature T_{aw} was measured with model 5 by leaving the model in the airstream until steady-state conditions prevailed. In this way, values of the recovery factor were obtained as a function of the local Reynolds number.

For the constant-temperature model a similar procedure was followed, except that the cover shielded the entire bismuth-tin plate and about

half of the leading-edge reinforcement. The cover was released immediately after the model was in position. No effort was made to correct for the extraneous effects introduced by the leading-edge reinforcement.

The main sources of error associated with these techniques are due to longitudinal conduction in the plate and normal conduction to the backing material. Longitudinal heat conduction in the plate makes the heat-transfer coefficient evaluated by equation (1) appear to be higher than its true value. In order to keep this error small, the tests were limited to short times (less than 0.15 second). Heat conduction to the backing material (fiber glass plastic laminate) makes the heat-transfer coefficient calculated with equation (1) appear to be lower than its true value.

L
3
7
3

THEORY

Two theories were used for comparison with the present data. The skin-friction coefficient from Van Driest's turbulent flat-plate theory (ref. 5) was used in order to get the heat-transfer coefficient for a constant-temperature plate h_{is} through the modified Reynolds analogy of reference 6 $\left(N_{St} = 0.6c_f\right)$. Ferrari's theory (ref. 7) was used to predict the ratio

$$\frac{(h)_{\text{step wall temperature}}}{(h)_{\text{constant wall temperature}}} = \frac{h}{h_{is}}$$

It is shown in the appendix that this ratio is given by

$$\frac{h}{h_{is}} = \left[1 - K\left(\frac{l}{x}\right)^{\frac{4}{5}\frac{n+2}{n+1}}\right]^{-\frac{1}{n+2}} \qquad (x \gtrsim l) \qquad (2)$$

where n is the reciprocal of the exponent in the power law for the velocity profile in the boundary layer and K in this case is a function of l/x, Mach number, and T_w/T_{aw} (fig. 3) whereas for the incompressible turbulent boundary layer over a flat plate $K = 1$. However, for $0.6 < \frac{T_w}{T_{aw}} < 1.4$, K can be assumed to take on the value of unity for a wide range of Mach numbers with an error in h/h_{is} of less than 2 percent. (See fig. 4.)

It is further shown in the appendix that, if the effect of the temperature step is approximated by assuming the boundary layer to begin

at the location of the step, that is, $h_{is}(x-l)$ is used rather than $h(x)$ given by equation (2), this assumption results in overestimating both the heat-transfer coefficient and its slope dh/dx. The error in heat-transfer coefficient, presented in figure 5, might not be prohibitively large for engineering applications. However, the error in slope given by

$$\frac{\frac{d}{dx} h_{is}(x-l)}{\frac{d}{dx} h(x)} = \frac{h_{is}(x-l)}{h(x)} \frac{10z \frac{x}{l}}{10z\left(\frac{x}{l} - 1\right) + \frac{\frac{x}{l} - 1}{\left(\frac{x}{l}\right)^{0.9} - 1}}$$

L
3
7
3

can be substantially larger.

For the present investigation, values of T_w/T_{aw} of about 0.95 were obtained, and equation (2) was used to predict the ratio h/h_{is} for $n = 7.5$.

EXPERIMENTAL RESULTS

There is definite evidence that the boundary-layer transition occurred very close to the leading edge. Values of the recovery factor measured with model 5 at several stations starting at 1 inch from the leading edge are plotted in figure 6 and they are seen to agree with previous experimental determinations for compressible turbulent boundary layers. (See refs. 8 and 9.) Location of natural transition was further determined by means of a sublimation technique for transition visualization described in reference 10. A typical pattern is shown on figure 7.

On the light of this evidence it was felt that there was no need to fix transition artificially on models 2 to 5. However, on model 1 a boundary-layer transition strip consisting of distributed three-dimensional roughness 0.003 inch high was located next to the leading edge. For the purposes of the present investigation, the boundary layer was assumed to be turbulent from the leading edge.

Pressure measurements showed that shock waves originating at the entrance of the channel (fig. 1) impinged on the model at about $x = 5$ inches and therefore only the data at $x < 5$ inches are presented.

Corrections Applied in Data Analysis

Two independent corrections were applied to the heat-transfer coefficient evaluated by equation (1) in order to compensate for the errors arising from longitudinal conduction in the plate and normal conduction to the backing.

The correction for longitudinal conduction was obtained by use of an unpublished method derived at the Gas Dynamics Branch of the Langley Research Center. This method assumes calorimetric heating across the plate and includes the effects of interference between aerodynamic heat transferred to the plate and heat conducted in the plate. The calculations were based on the measured gradient $\partial h/\partial x$ and they show that, for the times involved in the tests, the error for all models is about 4 percent for the first station (closest to the step) and decreases to less than 1 percent thereafter.

L
3
7
3

The correction for normal conduction to the backing material was calculated by using the exact solution for the transient aerodynamic heating of a semi-infinite composite slab. (See ref. 11.) This correction also accounts for the fact that the thermocouples were located at the bottom surface of the metal plate. Computations show that, for the testing times involved, the ratio of the measured heat-transfer coefficient to the corrected heat-transfer coefficient is a linear function of the parameter $h \frac{\delta}{k_{plate}}$ and varies from 0.77 to 0.83.

Analysis of Results

Figure 8(a) shows the measured, uncorrected heat-transfer coefficient at two typical pressure levels compared with the theoretically predicted values. Figure 8(b) shows the same values corrected for longitudinal conduction, normal conduction to the backing, and temperature difference across the plate. Model 1 varies appreciably from the rest of the models and these variations are attributed to the fact that this particular model was extensively used in preliminary runs and was somewhat damaged. Good agreement with theory is found in the data of models 2 and 3. Increases of up to 90 percent in the heat-transfer coefficient were observed as a consequence of the wall-temperature step. Isothermal-model data appear to be consistently lower than theory by about 10 percent except for stations at 4.5 and 5 inches which might be influenced by the shock pattern. Since the same sources of systematic measurement errors are present in all models, the possibility of a similar error in the data of models 1, 2, and 3 cannot be ruled out; it is felt, however, that, even if this is the case, the present conclusions are true.

Figure 9(a) shows a nondimensional plot of all the data, corrected for heat-conduction effects, compared with Van Driest's theory. Model 4 is at an essentially constant wall temperature whereas models 1, 2, and 3 include the effects of the wall-temperature step. A broken line has been faired through the data of model 2 at three pressure levels. It can be seen that these data do not follow the trend of the isothermal model (model 4) and they do not correlate at different presssure levels. This effect is present, to a greater or lesser degree, in all nonisothermal models. In figure 9(b) the values of the Nusselt number of figure 9(a) for models 1, 2, and 3 have been reduced to constant wall-temperature conditions by multiplying the Nusselt number by the ratio h_{is}/h given by equation (2). This reduced Nusselt number has been found to be in generally good agreement with the isothermal-plate theory, and it allows correlation of the data obtained at different Reynolds numbers.

L
3
7
3

CONCLUSIONS

An experimental investigation has been conducted at a Mach number of 2 to determine the effects of a step in wall temperature upon the heat-transfer characteristics of a turbulent, compressible boundary layer along a flat plate under near-equilibrium conditions $\left(\frac{T_w}{T_{aw}} \approx 0.95\right.$ where T_w is the wall temperature and T_{aw} is the adiabatic wall temperature$\left.\right)$.

An analysis of presently available theories yields the following conclusions:

1. When the wall-temperature distribution on a flat plate having a turbulent boundary layer consists of a step function with the step located at a distance l from the leading edge, the heat-transfer coefficient presents a theoretically infinite discontinuity at $x = l$ and gradually decreases thereafter according to the law

$$\frac{h}{h_{is}} = \left[1 - K\left(\frac{l}{x}\right)^{\frac{4}{5}\frac{n+2}{n+1}}\right]^{-\frac{1}{n+2}} \qquad (x \geqq l)$$

where

h heat-transfer coefficient for step-temperature distribution

h_{is} heat-transfer coefficient for constant-temperature distribution

n reciprocal of exponent in power law for boundary-layer velocity profile

l distance from leading edge to temperature step

x longitudinal coordinate from leading edge

For incompressible flow $K = 1$ and for compressible flow K is a function of l/x, Mach number, and T_w/T_{aw}. However, for $0.6 < \frac{T_w}{T_{aw}} < 1.4$ and supersonic flow, a value of $K = 1$ can be assumed with an error in h/h_{is} of less than 2 percent.

L
3
7
3

2. This law has been validated in incompressible flow by several investigators.

3. According to this law the heat-transfer coefficient falls off to within 10 percent of the constant wall-temperature value h_{is} at a distance $x = 1.8l$ from the leading edge.

4. The $h(x)$ distribution represented by the preceding equation is similar to the $h_{is}(x-l)$ distribution, that is, the heat-transfer coefficient that would exist on an isothermal plate with the leading edge at the location of the step. However, the use of $h(x)$ from the preceding equation yields lower values of the heat-transfer coefficient and the slope dh/dx than would be obtained by the use of $h_{is}(x-l)$.

The experimental results of the present investigation, after suitable corrections were introduced to allow for heat-conduction effects, show satisfactory agreement with the theoretical equation for $K = 1$, a maximum increase in the heat-transfer coefficient of 90 percent having been measured near the wall-temperature step.

Langley Research Center,
National Aeronautics and Space Administration,
Langley Field, Va., August 17, 1959.

APPENDIX

ANALYSIS OF THEORIES PREDICTING HEAT TRANSFER WHEN A WALL-TEMPERATURE STEP IS PRESENT

The problem of a stepwise wall-temperature distribution on a flat plate having a turbulent boundary layer has been treated theoretically and experimentally by several authors for incompressible flow. (See refs. 1 to 4.) The most recent work is the analysis of Reynolds, Kays, and Kline (ref. 4) which includes a review of past work and can be summarized by the equation

L
3
7
3

$$\frac{h}{h_{is}} = \left[1 - \left(\frac{l}{x}\right)^{\frac{4}{5}\frac{n+2}{n+1}}\right]^{-\frac{1}{n+2}} \qquad (x \geqq l)$$

For the present investigation Ferrari's theory (ref. 7) has been used to predict h/h_{is} in a turbulent compressible boundary layer. In the notation of this paper, Ferrari's formula can be written as:

$$\frac{N_{Nu}}{(N_{Nu})_{is}} = \frac{1}{(T_{aw} - T_w)_x}\left\{(T_{aw} - T_w)_{x=0} - \int_0^x \left[1 - \left(\frac{\xi\overline{c_f}(\xi)}{x\overline{c_f}(x)}\right)^{\frac{n+2}{n+1}}\right]^{-\frac{1}{n+2}} \frac{dT_w}{d\xi}\, d\xi\right\} \tag{A1}$$

where $\overline{c_f}(x) = \frac{1}{x}\int_0^x c_f(x)dx$, ξ is a dummy variable of integration, and $dT_w/d\xi$ represents the arbitrary wall-temperature distribution.

For the present case the integral in equation (A1) must be evaluated for a step wall-temperature function, and the following model is adopted:

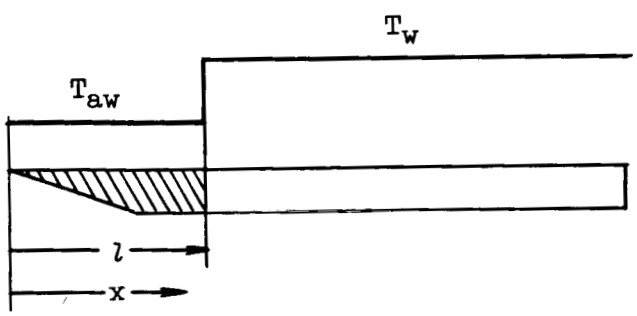

Under these conditions equation (A1) can be written as

$$\frac{N_{Nu}}{(N_{Nu})_{is}} = \frac{-1}{T_{aw} - T_w}\left\{\int_0^{l}\left[1 - \left(\frac{\xi\overline{c_f}(\xi)}{x\overline{c_f}(x)}\right)^{\frac{n+2}{n+1}}\right]^{-\frac{1}{n+2}}\frac{dT_w}{d\xi}\,d\xi\right.$$

$$+ (T_w - T_{aw})\left[1 - \left(\frac{l\overline{c_f}(l)}{x\overline{c_f}(x)}\right)^{\frac{n+2}{n+1}}\right]^{-\frac{1}{n+2}}$$

$$\left. + \int_l^{x}\left[1 - \left(\frac{\xi\overline{c_f}(\xi)}{x\overline{c_f}(x)}\right)^{\frac{n+2}{n+1}}\right]^{-\frac{1}{n+2}}\frac{dT_w}{d\xi}\,d\xi\right\}$$

Noting that for the present model $\frac{dT_w}{d\xi} = 0$ everywhere except at $x = l$, the latter reduces to

$$\frac{N_{Nu}}{(N_{Nu})_{is}} = \left[1 - \left(\frac{l\overline{c_f}(l)}{x\overline{c_f}(x)}\right)^{\frac{n+2}{n+1}}\right]^{-\frac{1}{n+2}} \qquad (x \geqq l) \qquad \text{(A2)}$$

The problem has now been reduced to the evaluation of $\overline{c_f}(l)$ and $\overline{c_f}(x)$. Although there is little doubt as to how to evaluate $\overline{c_f}(l)$ since the wall temperature is assumed to be constant for $0 < x < l$, a different matter is the evaluation of $\overline{c_f}(x)$ where the effects of the step in wall temperature should be included. As a first approximation, Ferrari neglected the effect of the step, that is, he assumed the wall temperature to have the constant value $T_w(x)$ everywhere and evaluated the local $c_f(x)$ with

$$c_f = 0.059R^{-1/5}\left(\frac{T_w}{T_\infty}\right)^{-0.432}$$

It may be noticed that this equation gives the skin-friction coefficient as a function of the cooling ratio but leaves out the Mach number dependency. Under these assumptions, Ferrari's result can be put in the form:

$$\frac{N_{Nu}}{(N_{Nu})_{is}} = \left[1 - K_1\left(\frac{l}{x}\right)^{\frac{4}{5}\frac{n+2}{n+1}}\right]^{-\frac{1}{n+2}} \qquad (x \geqq l)$$

where

$$K_1 = \left\{\left(\frac{l}{x}\right)^{\frac{4}{5}} + \left(\frac{T_w}{T_{aw}}\right)^{-0.432}\left[1 - \left(\frac{l}{x}\right)^{\frac{4}{5}}\right]\right\}^{-\frac{n+2}{n+1}} \tag{A3}$$

In the present paper an attempt has been made to bring in the Mach number dependency of K and in order to do so the Sommer and Short reference temperature T' (ref. 12) is introduced, which gives

L
3
7
3

$$c_f = 0.059R^{-1/5}\left(\frac{T'}{T_\infty}\right)^{-0.64} \tag{A4}$$

where

$$\frac{T'}{T_\infty} = 1 + 0.035M^2 + 0.45\left(\frac{T_w}{T_\infty} - 1\right)$$

provided the assumption is made that the viscosity of air is proportional to $(T)^{0.8}$.

Following Ferrari's lead of neglecting, as a first approximation, the effect of the step upon c_f, introduction of equation (A4) into equation (A2) yields after some manipulations

$$\frac{N_{Nu}}{(N_{Nu})_{is}} = \left[1 - K_2\left(\frac{l}{x}\right)^{\frac{4}{5}\frac{n+2}{n+1}}\right]^{-\frac{1}{n+2}} \qquad (x \geqq l)$$

where

$$K_2 = \left\{\left(\frac{l}{x}\right)^{\frac{4}{5}} + \left[\frac{1 + \dfrac{0.45}{1 + 0.035M^2}\left(\dfrac{T_w}{T_\infty} - 1\right)}{1 + \dfrac{0.45}{1 + 0.035M^2}\left(\dfrac{T_{aw}}{T_\infty} - 1\right)}\right]^{-0.64}\left[1 - \left(\frac{l}{x}\right)^{\frac{4}{5}}\right]\right\}^{-\frac{n+2}{n+1}} \tag{A5}$$

Values of $K_1\left(\frac{l}{x}, \frac{T_w}{T_{aw}}\right)$ and $K_2\left(\frac{l}{x}, \frac{T_w}{T_{aw}}, M\right)$ are shown in figure 3 for $n = 7.5$. (The Mach number range has been extended up to 8 to show trends only.) It may be seen that the variation of K due to Mach number M is small compared with the variation due to T_w/T_{aw}; therefore, the values

of $K_1\left(\frac{l}{x}, \frac{T_w}{T_{aw}}\right)$ from Ferrari's theory can be used instead of the more accurate $K_2\left(\frac{l}{x}, \frac{T_w}{T_{aw}}, M\right)$ provided the ratio h/h_{is} is not very sensitive to variations in K.

In order to evaluate the effect of K upon h/h_{is}, a plot of h/h_{is} is presented in figure 4 for several ratios T_w/T_{aw} using the values of $K_1\left(\frac{l}{x}, \frac{T_w}{T_{aw}}\right)$ of figure 3. For T_w/T_{aw} ranging from 0.6 to 1.4, a maximum difference of 2 percent is found in h/h_{is}. Therefore, the effect of Mach number on K can be neglected over a wide range; furthermore, K can be taken as 1 for at least $0.6 < \frac{T_w}{T_{aw}} < 1.4$ with a very small (2-percent) error in the predicted values of h/h_{is}.

The effect of the temperature step upon the heat-transfer coefficient can be roughly estimated by assuming the boundary layer to begin at the location of the step ($x = l$), that is, using $h_{is}(x-l)$ instead of $h(x)$. If this assumption is made and it is further assumed that

$$h_{is}(x) = (\text{Constant})\left(x^{-z}\right) \tag{A6}$$

as in reference 5, and

$$\frac{h(x)}{h_{is}(x)} = \left[1 - \left(\frac{l}{x}\right)^{\frac{9}{10}}\right]^{-\frac{1}{9}}$$

according to the preceding considerations; the following expression is obtained:

$$\frac{h_{is}(x-l)}{h(x)} = \frac{\left[1 - \left(\frac{l}{x}\right)^{\frac{9}{10}}\right]^{\frac{1}{9}}}{\left(1 - \frac{l}{x}\right)^{z}} \tag{A7}$$

which gives the theoretically predicted error when the boundary layer upstream of the step is neglected. Figure 5 shows a plot of equation (A7) as a function of x/l whereby it can be seen that neglecting the boundary layer ahead of the step results in overestimating the heat-transfer coefficient. This error is large in the immediate vicinity of the step but, if $z\left(M, \frac{T_w}{T_\infty}\right)$ is about 0.16 or less and $x > 1.1l$, the error is of

the order of 10 percent; therefore, $h_{is}(x-l)$ might be used as a convenient engineering approximation for $h(x)$. However, this approximation gives a substantially larger error in the slope dh/dx since

$$\frac{\frac{d}{dx}\, h_{is}(x-l)}{\frac{d}{dx}\, h(x)} = \frac{h_{is}(x-l)}{h(x)} \; \frac{10z\,\frac{x}{l}}{10z\left(\frac{x}{l} - 1\right) + \dfrac{\frac{x}{l} - 1}{\left(\frac{x}{l}\right)^{0.9} - 1}}$$

L
3
7
3

REFERENCES

1. Scesa, Steve, and Sauer, F. M.: An Experimental Investigation of Convective Heat Transfer to Air From a Flat Plate With a Stepwise Discontinuous Surface Temperature. Trans. ASME, vol. 74, no. 7, Oct. 1952, pp. 1251-1255.

2. Rubesin, Morris W.: The Effect of an Arbitrary Surface-Temperature Variation Along a Flat Plate on the Convective Heat Transfer in an Incompressible Turbulent Boundary Layer. NACA TN 2345, 1951.

3. Johnson, Donald S.: Turbulent Heat Transfer in a Boundary Layer With Discontinuous Wall Temperature. Pub. No. 55 (OSR Tech. Note 55-289), Dept. of Aero., The Johns Hopkins Univ., Aug. 1955.

4. Reynolds, W. C., Kays, W. M., and Kline, S. J.: Heat Transfer in the Turbulent Incompressible Boundary Layer. II.- Step Wall Temperature Distribution. NASA MEMO 12-2-58W, 1958.

5. Lee, Dorothy B., and Faget, Maxime A.: Charts Adapted From Van Driest's Turbulent Flat-Plate Theory for Determining Values of Turbulent Aerodynamic Friction and Heat-Transfer Coefficients. NACA TN 3811, 1956.

6. Rubesin, Morris W.: A Modified Reynolds Analogy for the Compressible Turbulent Boundary Layer on a Flat Plate. NACA TN 2917, 1953.

7. Ferrari, Carlo: Determination of the Heat Transfer Properties of a Turbulent Boundary Layer in the Case of Supersonic Flow When the Temperature Distribution Along the Constraining Wall is Arbitrarily Assigned. Rep. No. CAL/CM-807 (Contract NOrd-14523), Cornell Aero. Lab., Inc., Mar. 1954. (Also available from ASTIA as ATI No. 66171.)

8. Stalder, Jackson R., Rubesin, Morris W., and Tendeland, Thorval: A Determination of the Laminar-, Transitional-, and Turbulent-Boundary-Layer Temperature-Recovery Factors on a Flat Plate in Supersonic Flow. NACA TN 2077, 1950.

9. Brevoort, Maurice J., and Arabian, Barbara D.: Summary of Experimental Heat-Transfer Measurements in Turbulent Flow for a Mach Number Range From 0.87 to 5.05. NACA TN 4248, 1958.

10. Main-Smith, J. D.: Chemical Solids as Diffusible Coating Films for Visual Indications of Boundary-Layer Transition in Air and Water. R. & M. No. 2755, British A.R.C., 1950.

11. Trimpi, Robert L., and Jones, Robert A.: Transient Temperature Distribution in a Two-Component Semi-Infinite Composite Slab of Arbitrary Materials Subjected to Aerodynamic Heating With a Discontinuous Change in Equilibrium Temperature or Heat-Transfer Coefficient. NACA TN 4308, 1958.

12. Sommer, Simon C., and Short, Barbara J.: Free-Flight Measurements of Turbulent-Boundary-Layer Skin Friction in the Presence of Severe Aerodynamic Heating at Mach Numbers From 2.8 to 7.0. NACA TN 3391, 1955.

L
3
7
3

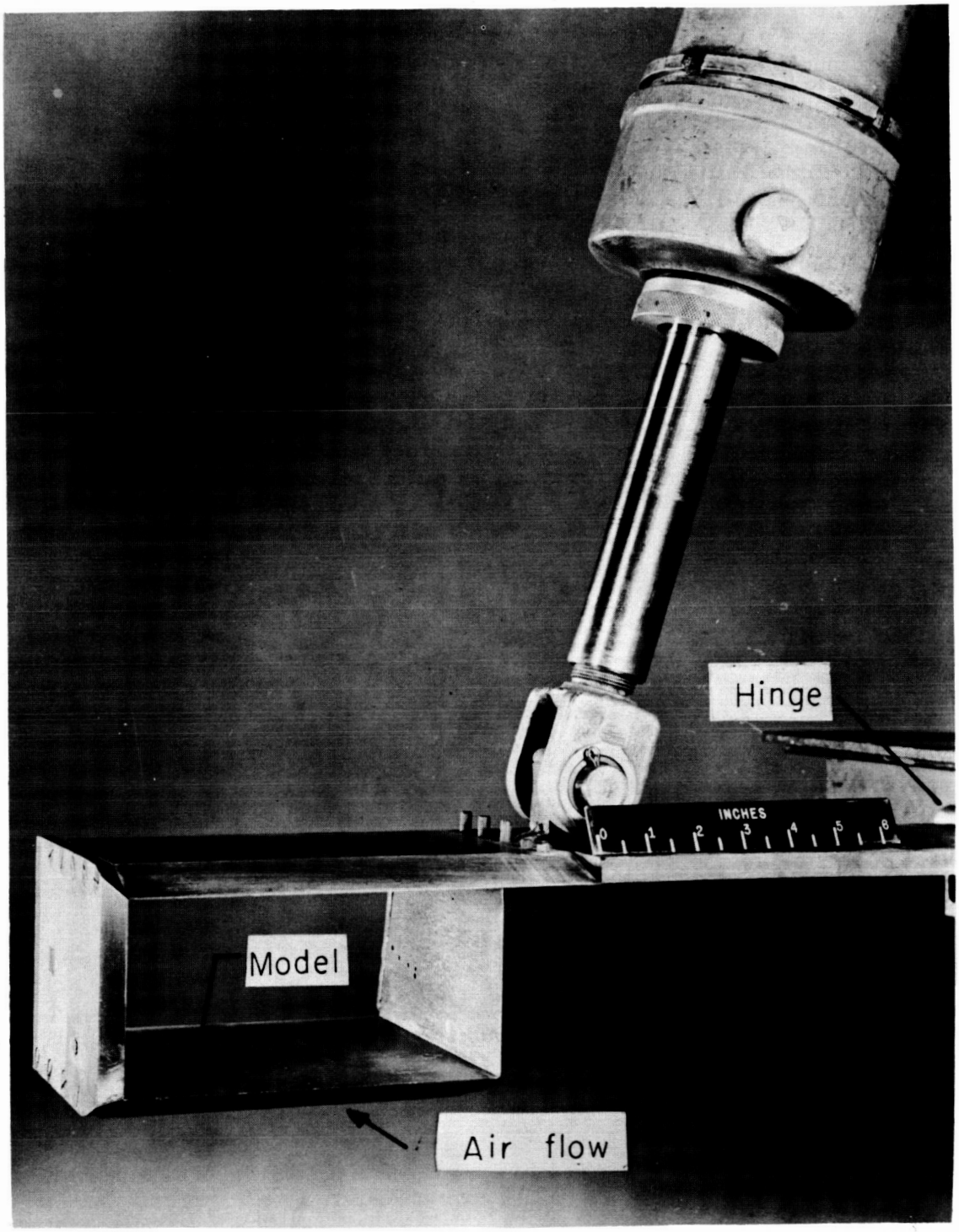

Figure 1.- Model and injection mechanism. L-58-862a.1

L-373

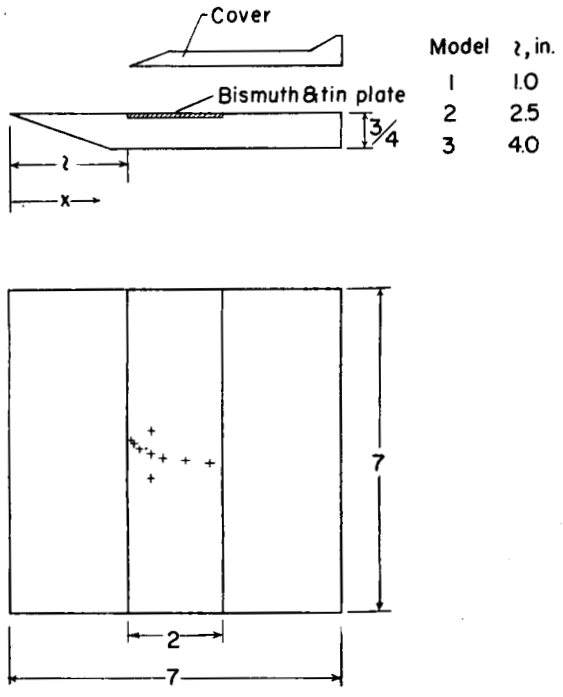

Model	ℓ, in.
1	1.0
2	2.5
3	4.0

Station	x − ℓ, in
1	.0625
2	.125
3	.250
4, 5, 6	.500
7	.750
8	1.250
9	1.750

(a) Models 1, 2, and 3; discontinuous temperature.

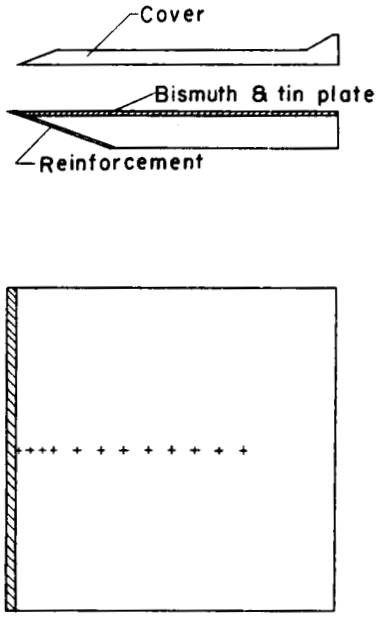

Station	x, in.	Station	x, in.
1	.25	7	2.50
2	.50	8	3.00
3	.75	9	3.50
4	1.00	10	4.00
5	1.50	11	4.50
6	2.00	12	5.00

(b) Model 4; constant temperature.

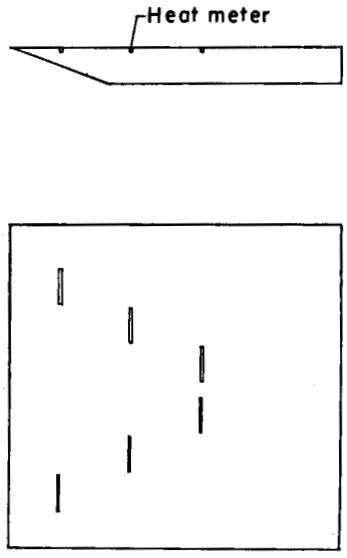

Station	x, in.
1,2	1.0
3,4	2.5
5,6	4.0

(c) Model 5; recovery temperature.

Figure 2.- Models.

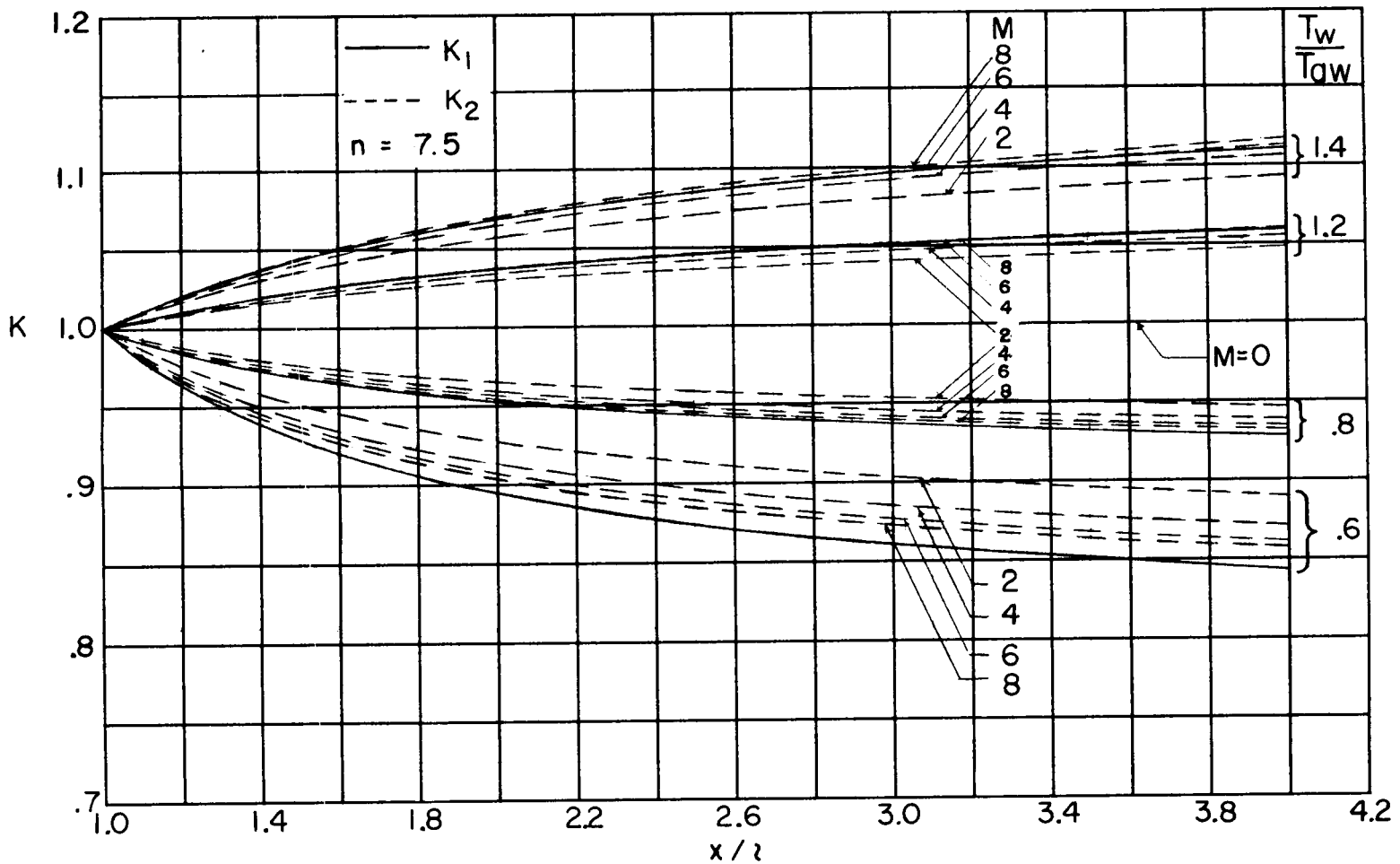

Figure 3.-Values of K_1 and K_2.

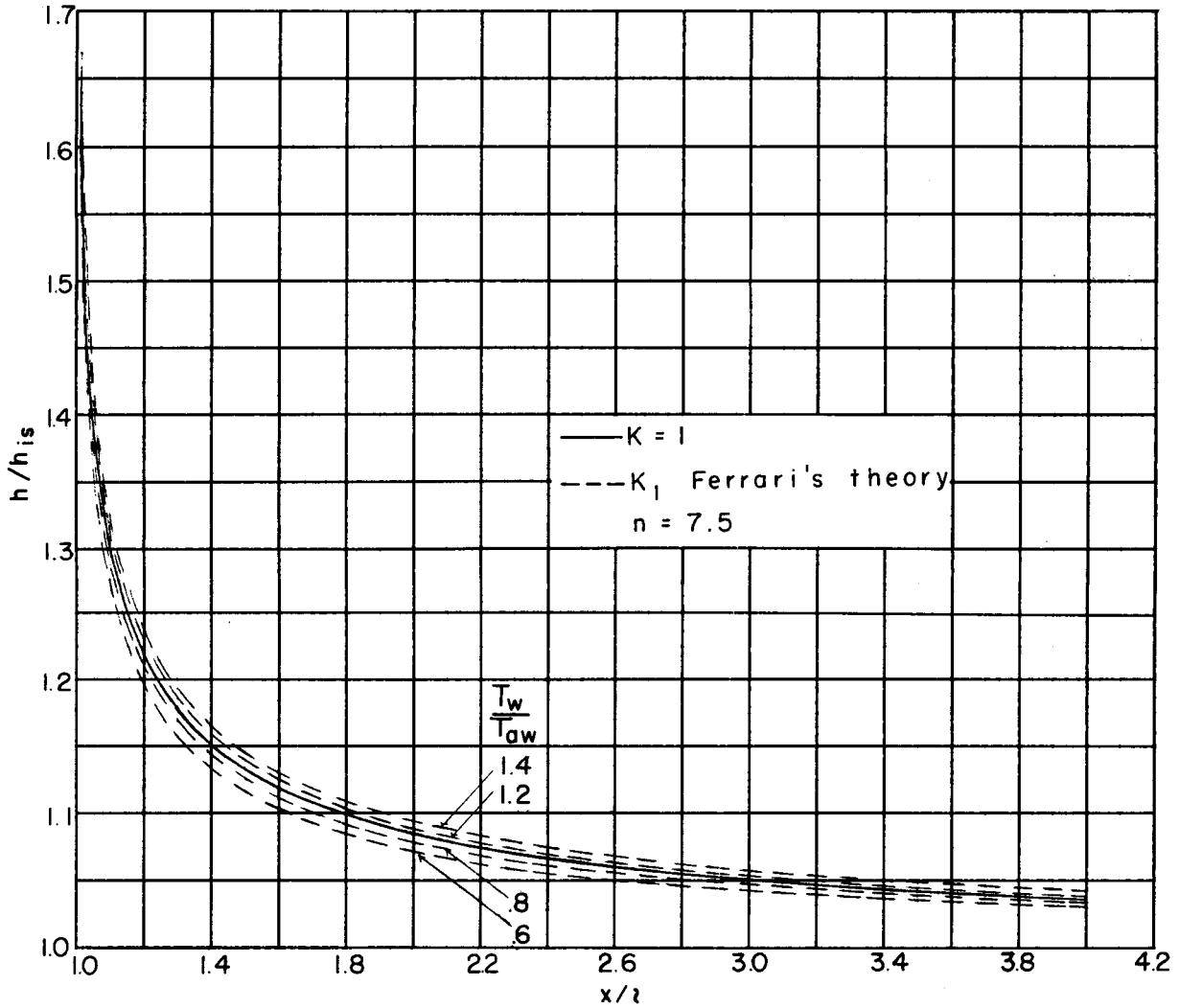

Figure 4.- Values of $\frac{h}{h_{is}}$ for $K = 1$ and K_1 from figure 3 at several values of $\frac{T_w}{T_{aw}}$.

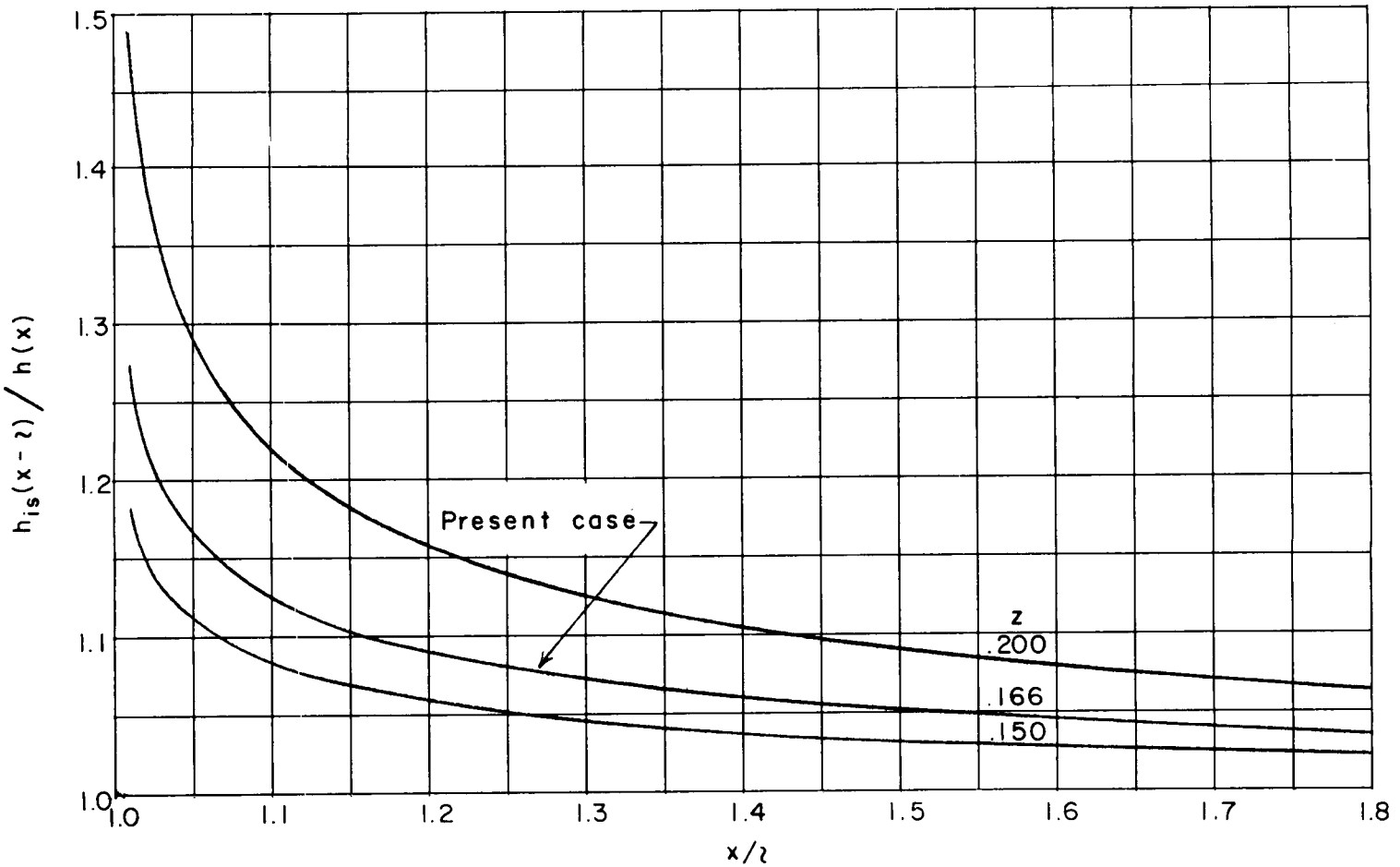

Figure 5.- Error involved in approximation $h(x) = h_{is}(x - l)$. $h_{is}(x - l) = (\text{Constant})(x - l)^{-z}$.

$$z = z\left(M, \frac{T_w}{T_\infty}\right).$$

L-373

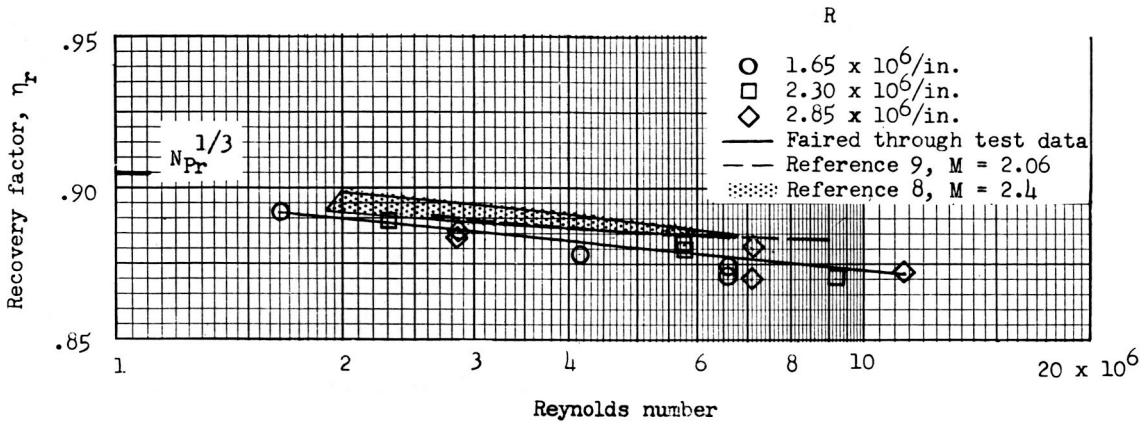

Figure 6.- Recovery factor.

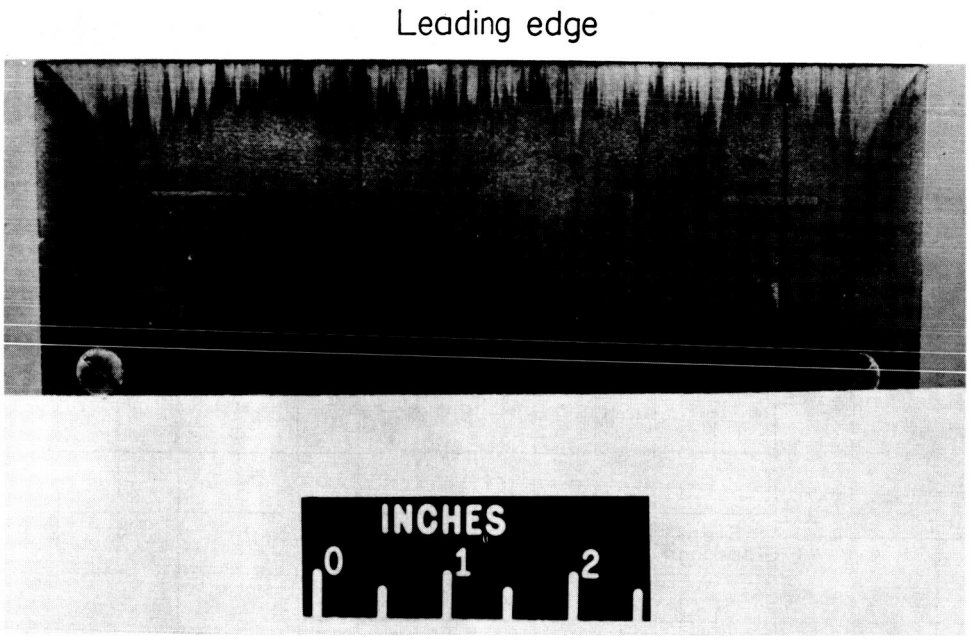

L-58-4047.1

Figure 7.- Pattern of acenapthalene crystals after a 10-second run showing boundary-layer transition near leading edge.

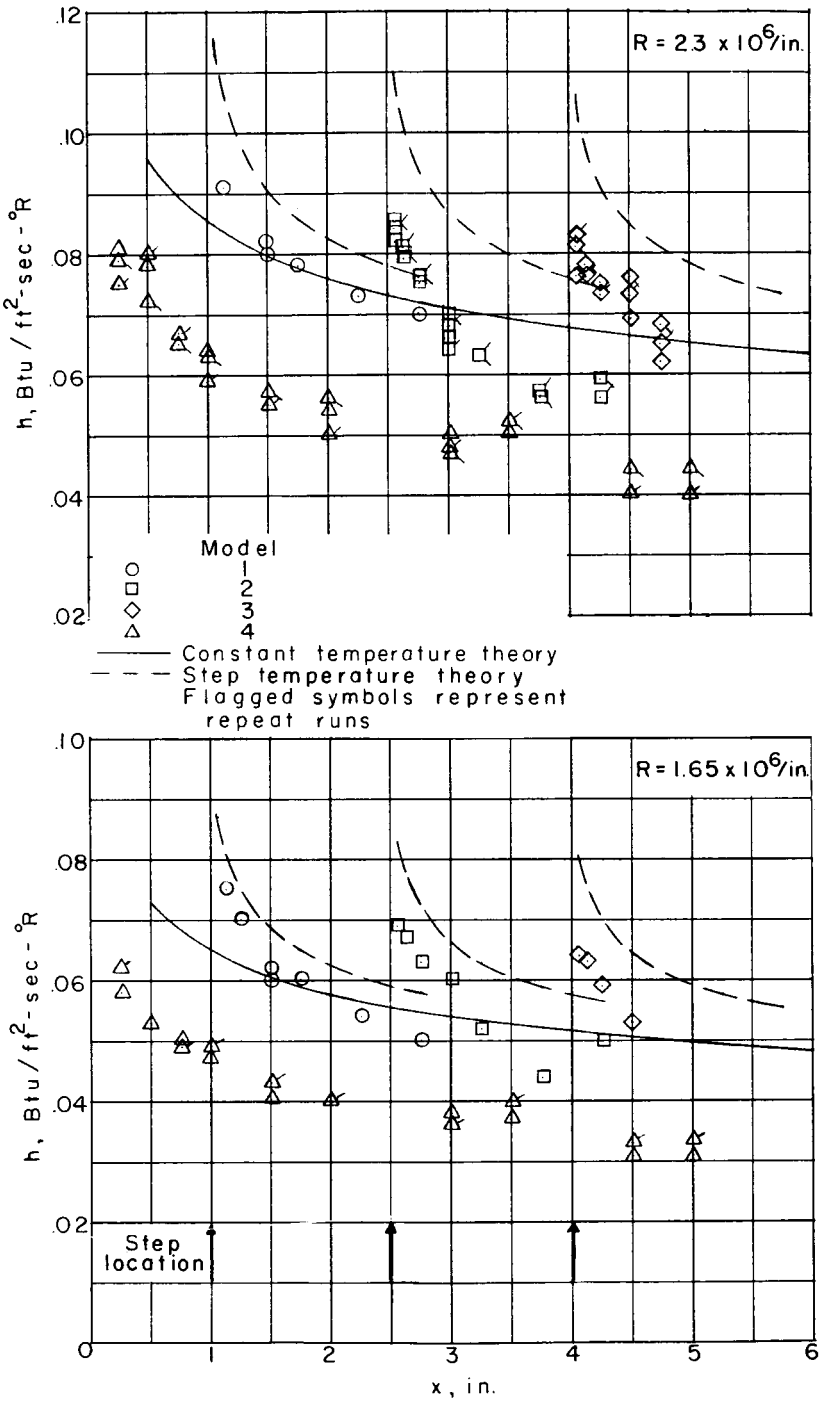

(a) Uncorrected values.

Figure 8.- Heat-transfer coefficient.

L-373

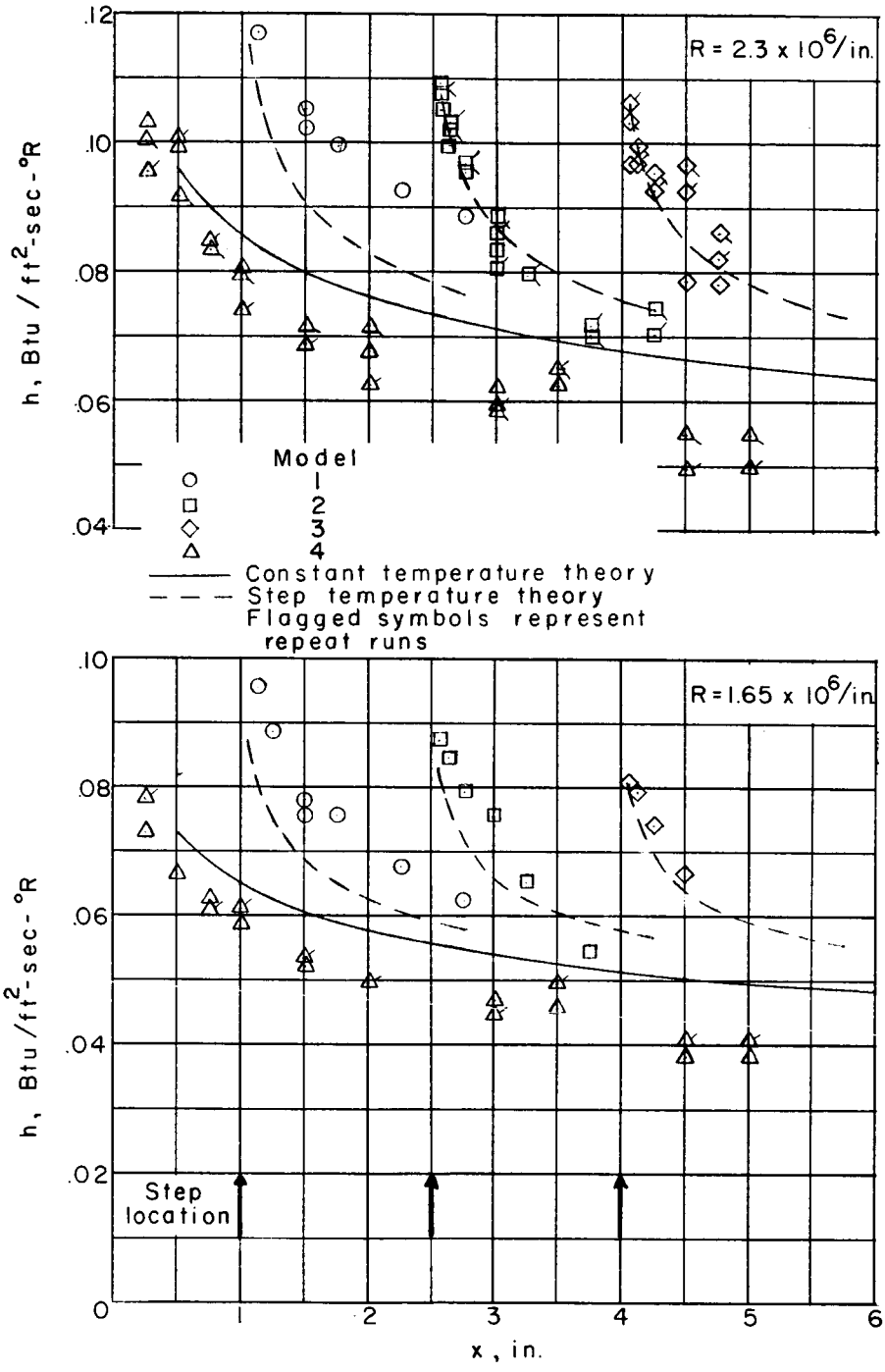

(b) Corrected values.

Figure 8.- Concluded.

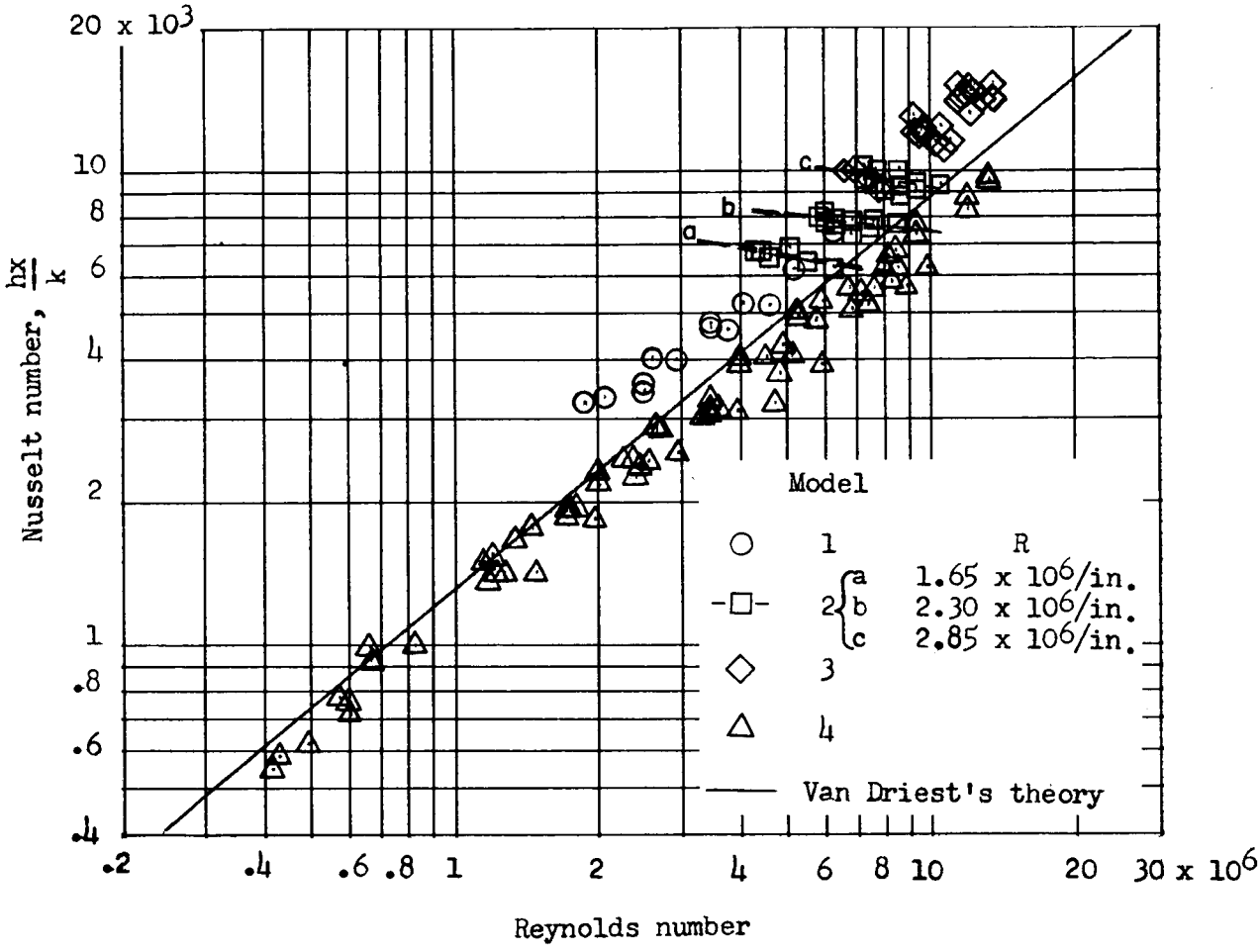

(a) Corrected Nusselt number.

Figure 9.- Nusselt number. $M = 2$; $N_{Pr} = 0.74$.

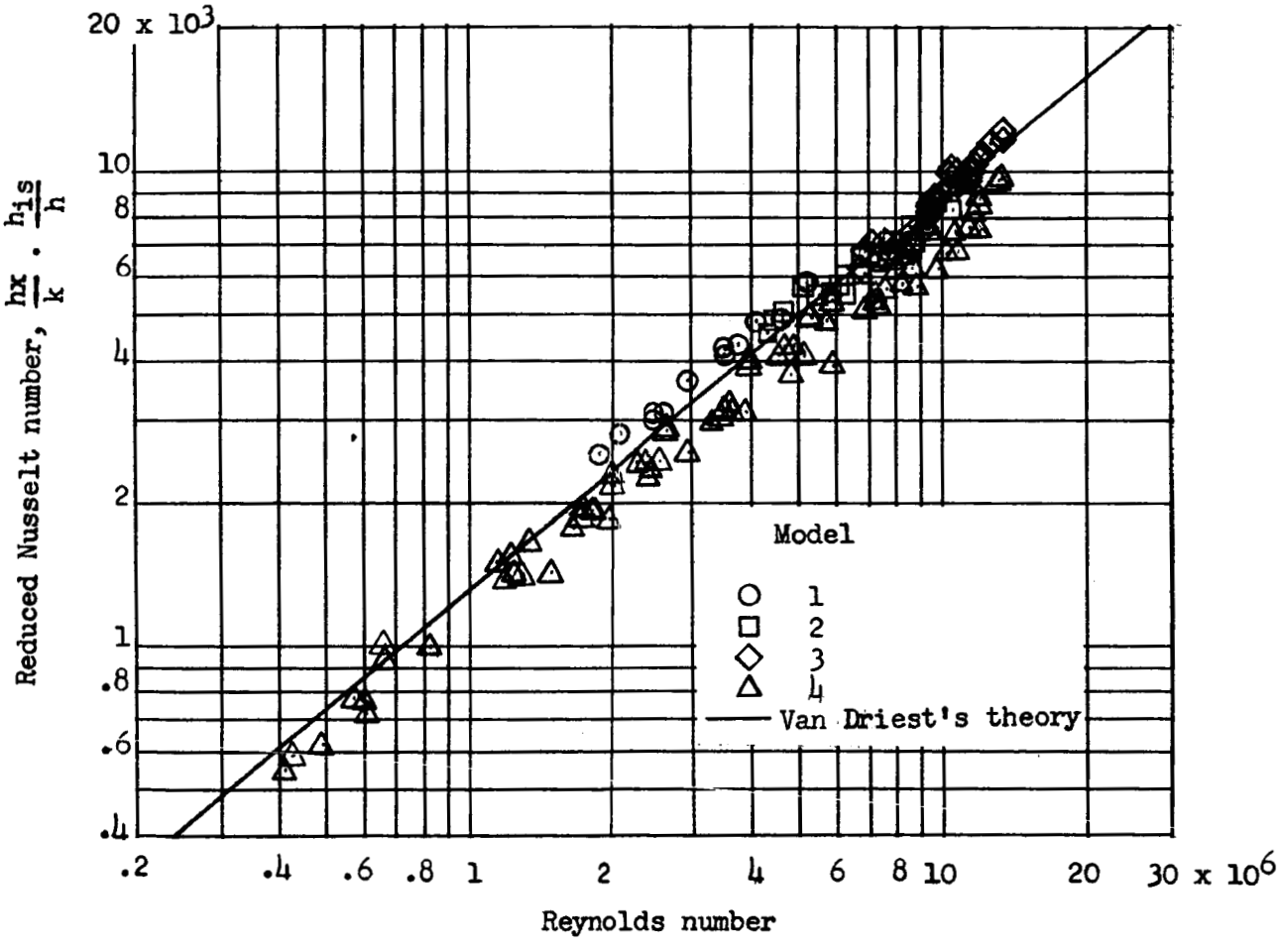

(b) Corrected Nusselt number reduced to isothermal wall conditions.

Figure 9.- Concluded.